Hydrogeology Journal (2014) 22: 175–187
DOI 10.1007/s10040-013-1059-z

Thermal tracer testing in a sedimentary aquifer: field experiment (Lauswiesen, Germany) and numerical simulation

Valentin Wagner · Tao Li · Peter Bayer · Carsten Leven · Peter Dietrich · Philipp Blum

Abstract An active and short-duration thermal tracer test (TTT) was conducted in a shallow sedimentary aquifer at the Lauswiesen test site, near Tübingen, Germany. By injecting 16 m^3 of warm water at 22°C, a thermal anomaly was created, which propagated along the local groundwater flow direction. This was comprehensively monitored in five observation wells at a few meters distance. The purpose of this well-controlled experiment was to determine the practicability of such a TTT and its suitability to examine hydraulic characteristics of heterogeneous aquifers. The results showed that the thermal peak arrival times in the observation wells were consistent with previous observations from alternative field testing such as direct-push injection logging (DPIL). Combined analysis of depth-dependent temperatures and peak arrival times, and comparison with a numerical heat transport model, offers valuable insights into the natural flow field and spatial distribution of hydraulic conductivities. The study was able to identify vertical flow focusing and bypassing, which are attributed to preferential flow paths common in such sedimentary sand and gravel aquifers. These findings are fundamental for further development of experimental designs of active and short-duration TTTs and provide a basis for a more quantitative analysis of advective and conductive transport processes.

Keywords Tracer tests · Heat transport · Direct-push injection logging (DPIL) · Germany · Thermal conditions

Received: 11 February 2013 / Accepted: 17 September 2013
Published online: 16 November 2013

Published in the theme issue "Hydrogeology of Shallow Thermal Systems"

V. Wagner (✉) · P. Blum
Karlsruhe Institute of Technology (KIT),
Institute for Applied Geosciences (AGW), Kaiserstr. 12,
76131, Karlsruhe, Germany
e-mail: valentin.wagner@kit.edu
Tel.: +49-721-608-45065
Fax: +49-721-606-279

T. Li
Institute for Geology,
Leibniz University Hannover, Callinstr. 30, 30167,
Hannover, Germany

P. Bayer
ETH Zurich, Geological Institute,
Sonneggstr. 5, 8092, Zurich, Switzerland

C. Leven · P. Dietrich
Center for Applied Geoscience (ZAG),
University of Tübingen,
Sigwartstr. 10, 72076, Tübingen, Germany

P. Dietrich
Department of Monitoring and Exploration
Technologies (MET), UFZ,
Helmholtz Centre for Environmental Research,
Permoserstr. 15, 04318, Leipzig, Germany

Introduction

For decades, heat has been considered as a groundwater tracer. However, despite the positive experience from several field tests and a range of different applications, it is still not routinely used in this context in hydrogeology. Anderson (2005) and Saar (2011) have presented comprehensive reviews of heat as a tracer. Recently, interest has been growing, particularly in using natural temperature variability to characterize aquifer/surface-water interactions (Doussan et al. 1994; Conant 2004; Schmidt et al. 2006; Keery et al. 2007; Constantz 2008; Vogt et al. 2010; Molina-Giraldo et al. 2011b), to reveal climate-change effects (e.g. Taniguchi et al. 1999; Brouyère et al. 2004), for localization of preferential flow paths or fractures (e.g. Leaf et al. 2012; Pehme et al. 2013), and to trace back direct anthropogenic influences (e.g. Ferguson and Woodbury 2007; Engelhardt et al. 2013; Menberg et al. 2013). Further studies concentrated on temperature-depth profiles to estimate vertical heat flux, vertical groundwater flux and thermal aquifers properties (e.g. Taniguchi et al. 2003; Lowry et al. 2007; Kollet et al. 2009).

Natural temperature variability has especially been in focus when pronounced and measurable over long periods of time, for example, as vertical temperature profiles in a streambed, or as observed in seasonal or diurnal temperature fluctuations of groundwater. Such long-term time series can serve as important information to more reliably simulate processes in aquifers on different scales. For example, Bravo et al. (2002) applied groundwater temperatures to constrain parameter estimation in a groundwater flow model of a wetland system. Rath et al. (2006) and Jardani and Revil (2009) used synthetic test cases to demonstrate the usability of temperature measurements for numerical groundwater model inversion.

Significant and abrupt change of temperature in aquifers is not common in nature. In contrast, artificially generated cold or hot temperature anomalies, which can be caused by geothermal energy utilization, often exhibit such a pronounced and abrupt change. Several injection-storage experiments have been performed in the past, mainly deployed to examine the performance of aquifer thermal storage systems (ATES, e.g. Sauty et al. 1982b; Molz et al. 1983; Xue et al. 1990; Palmer et al. 1992; Kocabas 2005; Wu et al. 2008). Such experiments are commonly conducted with large volume injections of hot water (thousands of m^3) and with monitoring of aquifer temperature changes over a relatively long duration (months to years). The main objectives of such field tests are the assessment of hot-water storage capacity and/or recovery efficiencies in the target aquifer and model validation to simulate ATES (e.g. Ziagos and Blackwell 1986; Xue et al. 1990; Molson et al. 1992).

Sauty et al. (1982a, b) conducted a series of aquifer storage experiments with single and doublet-well configurations and injection volume of 245–1,680 m^3 at the Bonnaud site in France. The temperature measurements were used to calibrate two numerical models. Palmer et al. (1992) performed a heat injection experiment at the Borden site in Canada, to investigate the feasibility of storing thermal energy in shallow unconfined aquifers near the water table. In a companion study, Molson et al. (1992) successfully validated a three-dimensional (3D) density-dependent numerical flow and transport model using the Borden field data. They demonstrated that processes of heat convection, dispersion, diffusion, retardation, buoyancy and boundary heat loss can be represented by their model. They also emphasized the importance of the vertical surface-heat loss mechanism when long-term thermal storage is concerned near the water table. Shook (1999, 2001) suggested predicting temperature signals from conservative tracer breakthrough curves (BTC) through variable transformation, for example, by applying thermal retardation factors. This was demonstrated for homogeneous test cases and for heterogeneous conditions when thermal conduction and dispersion can be neglected as second-order effects.

When using heat as a tracer, there is another type of application, called ‘thermal tracer test’ (TTT) or active TTT (e.g. Leaf et al. 2012). The utilization of TTT is mainly for aquifer characterization, in which warm (or cold) water is injected as a tracer into the aquifer and then temperature changes are measured in the injection well and/or in nearby observation wells. These tests are different from the aforementioned studies for thermal storage in injection volume and experimental scale, as well as duration (normally only for a few days in TTT, Table 1). Keys and Brown (1978) presented a field study of TTT in the High Plains of Texas, USA. They conducted three artificial recharge experiments with various injection water volumes and rates. The recharged water was supplied from a lake, where the water temperature fluctuated between 13 and 23°C, and provided thermal pulses recorded in the groundwater temperature logs. By evaluating the thermal pulses they identified contrasts in the horizontal groundwater velocity of the studied area. Macfarlane et al. (2002) reported an injection/pumping experiment in west-central Kansas, USA. They injected about 360 m^3 of heated water (73°C) at one well and then pumped from the other well at about 13 m distance. A distributed optical-fiber temperature-sensing device (DTS) was used for monitoring the temperature changes under transient conditions, and vertical temperature profiles were recorded from the production well. This study estimated a groundwater velocity from the temperature profiles, which was comparable to that derived from previous pumping tests. DTS was also applied in recent related work by Leaf et al. (2012), who examined a porous fractured sandstone aquifer using open-well thermal dilution tests in two wells near Madison, Wisconsin, USA. Their tests only provided information on the borehole flow regimes and not on the spatial heterogeneity of the aquifer. They demonstrated that DTS measurements are a suitable alternative to standard heat pulse methods or spinner flow meters. Read et al. (2013) presented a TTT in a fractured aquifer at the Ploemeur site in Brittany, France (Table 1). They determined a pronounced retardation of the BTC in a monitoring well compared to the one of a solute tracer. Read et al. (2013) explained this observation by the stronger fracture-matrix interaction of the thermal tracer.

Vandenbohede et al. (2008a, b) reported their experience from two single-well push-pull tests, which they conducted in a deep aquifer in the Belgian coastal plain. The tests were designed to evaluate the performance of a planned ATES, but the data were further interpreted to study the differences between solute and heat transport in Vandenbohede et al. (2008a). The temperature of the injected water for both tests was about 11.5°C, and slightly colder compared to the ambient aquifer temperature of 15.8°C. The tests, including injection, rest and extraction phase were performed in periods of 9–22 days, with rates of a few m^3 per hour. A numerical model was adopted to simulate the field tests (Vandenbohede et al. 2008a). After comparing the simulated results on solute (chloride) and heat transport, they concluded that for a push-pull test, the most sensitive parameter in solute transport is solute longitudinal dispersivity and in heat transport it is thermal diffusivity. Ma et al. (2012) applied a numerical model of a complex aquifer–river system to discuss the role of variable density and viscosity assumptions on heat transport modeling (Table 1). They observed that up to a maximum temperature difference of 15°C in the model domain, the assumption of constant fluid density and viscosity appears to have only minor effect on the simulated temperature distribution (Ma and Zheng 2010). They also state that this is valid for any heat transport model and for various field conditions. All studies on TTT successfully demonstrated that aquifer structures and/or properties can be evaluated from monitoring groundwater

 DOI 10.1007/s10040-013-1059-z

Table 1 Overview of active, short term (<12 days) thermal tracer tests reported in the literature

Location	Aquifer type	Injected volume (m^3)	Injection rate ($m^3\ h^{-1}$)	Temperature difference (K)	Injection time (h)	Duration (days)	Observation wells	Remarks	Reference
Stewart site, Texas, USA	Unconsolidated porous aquifer	32,832	3,283	−2.3 to +7.7	240	10	5	Natural gradient test; variable injection temperature	Keys and Brown (1978)
Bonnaud site, France	Confined porous aquifer	245-1,680	2.9-7.5	≈ +18 to 25	72-480	8-184	11	Seven experiments: single-, doublet-, cyclic-type	Sauty et al. (1982b)
Kansas, USA	Porous fractured sandstone aquifer	359.6	2.5	+55	173	7.2	1	Forced gradient test, one production and one observation well	Macfarlane et al. (2002)
Coastal plane, Belgium	Deep fine sand confined porous aquifer	188	3.9	−4.3	48.15	9.2	–	Only short term push and pull test	Vandenbohede et al. (2009)
Hanford site, USA	Unconfined and unconsolidated porous aquifer	156	16.3	−7.8	9.75	11.8	28	Parallel solute and thermal tracer test	Ma et al. (2012)
Wisconsin, USA	Porous fractured sandstone aquifer	Not specified	0.6-0.8	+2 to 7	2.6-3	0.2-0.3	–	Three open-well thermal dilution tests; wells intersect several aquifers	Leaf et al. (2012)
Ploemeur site, France	Fractured aquifer	32.1	2.1	≈ +35	11	0.67	1	Forced gradient test, one production and one observation well	Read et al. (2013)
Lauswiesen site, Germany	Unconfined shallow porous aquifer	16	2.0	+11	8.0	4	5	Natural gradient test	This study

temperatures. However, active TTT is still not a standard method for aquifer testing.

The current study examines viability and usability of the TTT for characterization of a shallow heterogeneous aquifer at the Lauswiesen test site close to Tübingen, Germany. An active, small-scale and short-term TTT was performed with warm water injection in the well-known unconfined porous aquifer (Table 1), and the resulting temperature anomaly was monitored in five downgradient observation wells. For the interpretation, well- and depth-specific temperature time series are evaluated with emphasis on maximum observed temperature changes and peak arrival times. A numerical flow and heat transport model is set up to simulate the experiment and identify effects from aquifer heterogeneity. The intention is to determine to what extent spatial hydraulic heterogeneity and density effects influence the thermal tracer propagation. This is complemented by comparison to the findings from an alternative field investigation, the direct-push injection logging (DPIL), at the same site (Lessoff et al. 2010).

Thermal tracer test set up at Lauswiesen site

Study site

The Lauswiesen test site is located near the city of Tübingen in southwest Germany (Fig. 1), where numerous investigations have previously been performed to study aquifer properties (e.g. Rein et al. 2004; Riva et al. 2006; Lessoff et al. 2010; Händel and Dietrich 2012). The test site is part of a heterogeneous alluvial aquifer located close to the Neckar River. The injection well is around 60 m away from the river. The aquifer consists of loosely packed Quaternary sandy gravel, overlain by Quaternary silty clay and clayey gravel. As observed in previous studies by Bou Ghannam (2006) and Schneidewind (2008), the aquifer can be divided into two major zones. The first zone reaches down to 6 m below land surface (bls) and consists of sand and gravel, with a small portion of fines. Based on these studies, it can be assumed that the first layer is relatively more homogeneous than the second layer, which ranges from 6 to 10 m bls. According to soil-sample analyses from Sack-Kühner (1996), the portion of fines increases in the lower part of the aquifer below 7 m bls. This lower part of the aquifer appears to be more heterogeneous with some lower-permeability zones and pronounced local anisotropies. The Lauswiesen aquifer is underlain by Triassic marl and clay stones (Middle Keuper), which form a natural aquitard. The water table at the site is about 4 m below surface, but can vary several decimeters due to the proximity of the Neckar River. The hydraulic gradient of Lauswiesen is estimated to be around 0.2–0.3%. The hydraulic conductivity of the aquifer was measured in several field campaigns using a variety of techniques, yielding average values in the range of K=2–3×10^{-3} m s^{-1} (Sack-Kühner 1996; Lessoff et al. 2010). Using a multilevel multi-tracer field experiment, Riva et al. (2006) determined an average effective porosity of 9.8% for the test site. Thus, the average and natural

 DOI 10.1007/s10040-013-1059-z

groundwater flow velocity towards the Neckar River is around 5.5 m day^{-1} at the site.

Thermal tracer test

The main groundwater flow axis through the chosen experimental area was determined from groundwater contour maps based on water-level measurements done over a 2-month period in existing monitoring wells, before the installation of the observation wells. The configuration of the wells for the TTT at the Lauswiesen site is outlined in Fig. 1. Thermal tracer injection was performed in a fully penetrating well, B2 (Table 2). For the tracer monitoring, five fully penetrating observation wells OW1–OW5, 1″ (2.5 cm) diameter, were installed along the pre-determined main groundwater flow axis with various spacing (Table 2). The reason of using small diameter observation wells for TTT was to minimize the effect of free convection within the well column, so that the measured fluid temperature in the observation wells could more accurately represent the temperature in the surrounding solid/fluid matrix (Leaf et al. 2012).

For the preparation of the thermal tracer, approximately 16 m^3 of groundwater were pumped out from the aquifer and then stored in a basin. As the experiment was conducted in summer time, during a warm weather period, the extracted water could be heated in the sun to about 22°C. Groundwater temperatures in the aquifer were continually monitored before the injection in every installed observation well and recorded, showing an average initial temperature T_0 of 11.02±0.30°C. Temperature measurements were acquired using chains of PT-100 thermistors (Platinum Thermometer, resolution 0.01°C). For each temperature chain, ten PT-100 sensors were attached with a spacing of 0.5 m to a transmission cable which was connected to a data reading unit (Fig. 2). Two temperature sensors (OW4; 7.2 m bls and OW5; 8.2 m bls) were damaged during the installation and therefore, both sensors were omitted for the experiment. During operation, measurements from each sensor were transmitted to a reading device at the land surface and recorded manually. The induced head changes from the injection were manually recorded in irregular time steps. The constant injection resulted in 3 cm of increase in hydraulic head at the injection well during the whole injection period.

During the injection period, the heated water was introduced as a thermal tracer from two injection units in B2 at 6 and 9 m bls, both with constant rates of 2×1 m^3 h^{-1} using two Grundfos MP1 pumps. Temperature changes were then monitored simultaneously in all observation wells and in the injection well B2. At the early phase of the experiment, measurements were taken more frequently (every 30 min). The injection ended after 8 h (0.33 days), while the temperature monitoring was continued until the end of experiment, which was terminated after about 100 h (4.2 days) after the start of injection.

Direct-push injection logging

Lessoff et al. (2010) applied the direct-push injection logging (DPIL; Dietrich et al. 2008) and direct-push slug test (DPST; Butler et al. 2002) for characterizing the spatial structure of hydraulic conductivity (K) at the Lauswiesen site test. They could demonstrate that the 258 measurements of relative conductivity (K_r) using DPIL are compatible with results from other more conventional methods performed at the site. All recorded DPIL–profiles (Fig. 3) are within a radius of 15 m around the injection well of the TTT. One DPIL–profile was directly obtained at the injection well and two profiles at the observation wells OW4 and OW5, which were also used for the TTT. The profiles are highlighted in Fig. 3 and will be compared to the TTT results of this study. All measured K_r values indicate that there is a significant difference in the hydraulic conductivities of the upper and lower part of the aquifer. A more detailed inspection of the profiles from B2, OW4 and OW5 reveals that the transition between the upper and the lower part of the

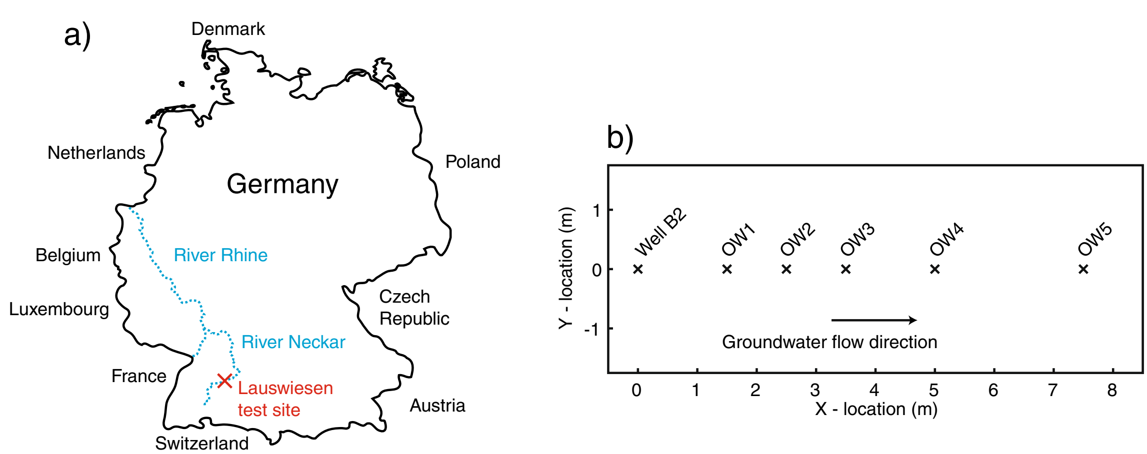

Fig. 1 **a** Location of the Lauswiesen test site, close to Tübingen, SW Germany. **b** Plan view of setup of the thermal tracer test. Well B2 (x=0, y=0) was used as injection well and OW1–OW5 served as observation wells during the test

 DOI 10.1007/s10040-013-1059-z

Table 2 Information on the wells used for the thermal tracer test at the Lauswiesen site

Well	Distance from the injection well B2 (m)	Screen length (m)	Inner well diameter (mm)	Material
B2	0.0	Fully screened	150	PVC[a]
OW1	1.5	6 (from bottom)	25	HDPE[b]
OW2	2.5	4 (from bottom)	25	HDPE[b]
OW3	3.75	4 (from bottom)	25	HDPE[b]
OW4	5.0	4 (from bottom)	25	HDPE[b]
OW5	7.5	4 (from bottom)	25	HDPE[b]

[a] Polyvinylchloride

[b] High-density polyethylene

aquifer is not at constant depth. Lessoff et al. (2010) deduced from the DPIL-profiles, that the upper part of the aquifer is more conductive and more homogenous than the lower part. Moreover, all three profiles show local maxima of K_r at certain depths (e.g. OW4 at a depth of 6.4 m bls, OW5 at a depth of 7.4 m bls).

Numerical model

Based on the existing knowledge of the Lauswiesen site, it is assumed that the subsurface can be represented by a layered unconfined aquifer with an underlying aquitard. A numerical model was set up using FEFLOW (Diersch 2009) to simulate the TTT with the injection of warm water in the aquifer and the transport of the heated groundwater through the sedimentary strata. Analogous to the TTT at the Lauswiesen site, the model contains five observation wells (Fig. 4). These are positioned in the center of the model domain, where the TTT is simulated. The total size of the numerical model is 130 m×26 m×15 m (width × height × depth), which is considered large enough to minimize boundary effects at the injection and observation wells. The total area is discretized with 30,656 triangle prismatic elements with an increasing resolution of the numerical mesh towards the well transect. The distance between the numerical nodes decreases from the model boundary to the well transect by a factor of 40.

The simulated stratified aquifer is separated in an upper and a lower part as suggested by the results of Lessoff et al. (2010). In the upper part of the aquifer, a free water table is simulated to account for a potential mound of the water table due to injection of water. This groundwater mound may affect the flow field, especially close to the injection well. Unsaturated-zone flow is calculated by applying the Richards equation, and the model allows for heat exchange between aquifer and unsaturated zone.

Fixed hydraulic heads are assigned at the inflow and outflow boundary of the model, and no flow at the remaining boundaries. The fixed heads are set to ensure a horizontal hydraulic gradient of 0.003 along the well transect and a depth below land surface of the water table of 4.0 m bls at B2 as measured before the TTT. On the upstream model boundary, a hydraulic head of 3.9 m bls is assigned and on the opposing site a value of 4.3 m bls. The temperatures of the inflowing groundwater and at the surface are similarly controlled by Dirichlet boundary conditions. The temperature of the inflowing groundwater and at all aquifer model edges is set to 11.0°C. This value was obtained from groundwater measurements before the TTT started. At the top of the model, the temperature is set fixed at 18.1°C, gradually declining to the groundwater temperature at the lateral unsaturated boundaries. This value was derived from linear extrapolation of temperature values obtained before the tracer injection in the section of the unsaturated zone (from the water table to 2.2 m bls).

The injection well, B2, is represented by a well module integrated in FEFLOW, which assigns a given extraction or injection rate to all nodes of the well. To realistically reproduce the conditions of the heated water injection, a combination of a temperature and the described well boundary condition is applied. For the injection phase (0–8 h), water is injected in the aquifer at a constant rate along the well screen. The

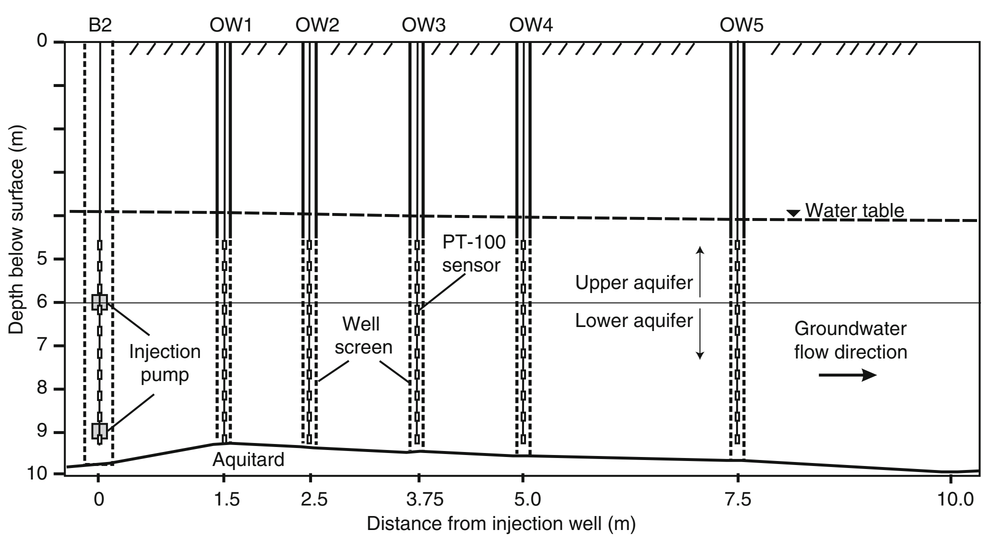

Fig. 2 Vertical cross-section along the well axis (x) showing positions of wells (B2, OW1–OW5), water table, aquifer and aquitard

 DOI 10.1007/s10040-013-1059-z

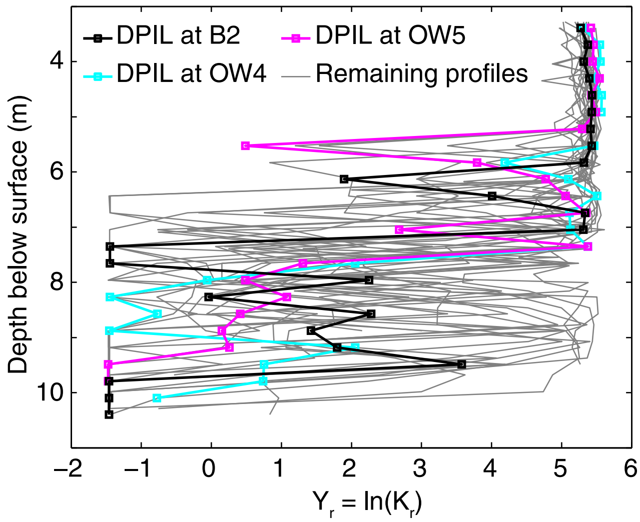

Fig. 3 Compound profiles of $Y_r = \ln(K_r)$ obtained from DPIL measurements within a radius of 15 m around the injection well of the TTT. The three DPIL profiles that are taken from observation wells also monitored during the TTT are highlighted. The DPIL measurements are extracted from the study of Lessoff et al. (2010)

temperature of the injected water is stated by a Dirichlet boundary condition. After the injection phase (>8 h after start of the injection), both boundary conditions referring to the injection well are deactivated.

Hydraulic and thermal parameters for the three model layers are subsequently calibrated by fitting simulated to measured temperatures during the TTT. The possible ranges of hydraulic conductivities of the three layers are derived from previous studies at this site. Lessoff et al. (2010) suggest an integral hydraulic conductivity of 3×10^{-3} m s^{-1}. Riva et al. (2006) compiled the results of several sieve analyses and determined different cluster groups with hydraulic conductivity values, K, between 3×10^{-4} and 5.9×10^{-3} m s^{-1}. These two values were

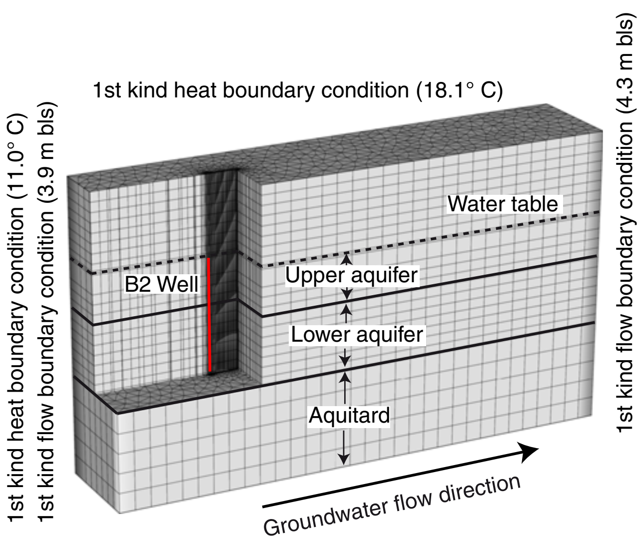

Fig. 4 Three-dimensional sketch of the model domain, numerical mesh, hydraulic and thermal boundary conditions. Values used as hydraulic and thermal boundary condition are specified in brackets

selected as initial assumptions for the two layers, with the upper aquifer layer being more conductive as the integral hydraulic conductivity parameter (3×10^{-3} m s^{-1}) suggested by Lessoff et al. (2010). A range of ±50% uncertainty is then defined for the calibration. Furthermore, it is assumed that the aquitard has a significantly lower hydraulic conductivity of 1.0×10^{-9} m s^{-1}. A constant effective porosity of 9.8%, as suggested by Riva et al. (2006), is set for the entire aquifer.

No measurements of the thermal conductivity and the heat capacity exist for the Lauswiesen test site. However, these parameters only show a small variability in sedimentary aquifers and may be well estimated by adopting values from other work: Parr et al. (1983), Palmer et al. (1992) and Markle et al. (2006) examined thermal properties of porous aquifers similar to the one at the Lauswiesen site. Based on the values and ranges reported therein, c_{pm}=2.8±0.3×10^6 J m^{-3} K^{-1} and λ_m=2.2±0.5 W m^{-1} K^{-1} were chosen. The thermal properties of the aquitard are estimated assuming a pure clay stone layer (Table 3). Volumetric heat capacities are derived from the study by Clauser (2011), and the corresponding thermal conductivity values are extracted from Domenico and Schwartz (1998). The longitudinal thermal dispersivity is estimated based on the empirical relationship by Neuman (1990)

$$\alpha_l = 0.017 L_s^{1.5} \tag{1}$$

where the travel distance L_s is considered to be the maximum distance between the source and the most distant observation well. The transversal dispersivity is set to one tenth of the longitudinal one (e.g. Molina-Giraldo et al. 2011a). For this TTT experiment, L_s, is 7.5 m and thus one derives a first estimate of α_L=0.34 m. Due to the substantial uncertainty in this parameter value, for the calibration, feasible ranges from 0 to 0.68 m are defined. Since mechanical thermal dispersion is not expected to be relevant for the diffusion-dominated transport in the aquitard, a small fixed value of α_L=0.01 m is set in the numerical model.

Evaluation methodology

The analysis of the recorded TTT data focuses on the development of the thermal plume and the governing transport processes in the porous aquifer. Injection of warm water induces a dynamically evolving thermal anomaly in the aquifer. The focus here is on the temperature change ΔT, which is determined by the difference between initial temperature and measured temperature values. Propagation of the warm water is seen in the wells using recorded thermal breakthrough curves (BTC). As diagnostics of the BTC, the maximal observed temperature change ΔT_{peak} and the peak arrival time t_{peak} were chosen. The ΔT_{peak} values are determined by scanning each measured temperature curve for the global temperature maximum. Thus, the peak arrival time t_{peak} is the corresponding point of time for which the

DOI 10.1007/s10040-013-1059-z

Table 3 Hydraulic and thermal parameter ranges applied for the numerical simulation. Values in *italic* are used to generate the numerical results that are further analyzed

		Hydraulic conductivity K (m s^{-1})		Volumetric heat capacity c_{pm} (J m^{-3} K^{-1})	Thermal conductivity λ_m (W m^{-1} K^{-1})	Longitudinal dispersivity α_l (m)
		Lower part	Upper part			
Aquifer (and gravel)	Min	1.5×10^{-4}	3.0×10^{-3}	*2.5×10^{6}*	1.7	0.01
	Median	3.0×10^{-4}	5.9×10^{-3}	2.8×10^{6}	2.2	0.34
	Max	*4.5×10^{-4}*	*8.9×10^{-3}*	3.1×10^{6}	*2.7*	*0.68*
Aquitard (clay stone)	Min	1.0×10^{-9}		2.3×10^{6}	1.1	0.01
	Median	*1.0×10^{-9}*		*2.3×10^{6}*	*1.1*	*0.01*
	Max	1.0×10^{-9}		2.3×10^{6}	1.1	0.01

temperature maximum is detected. According to Bellin and Rubin (2004), evaluation of t_{peak} has several advantages for examining tracer BTCs. It is not so much interfered by infrequent sampling, and the lack of early or late parts of the signal or measurements below the detection level is not as problematic as it is for the analysis of moments of the BTC. These interferences, which could hamper BTC interpretation, are also seen as critical for the TTT at the Lauswiesen site.

The influence of different transport processes can be quantified by dimensionless numbers. To analyze the ratio between advection and thermal conduction, the macroscopic Peclet number is defined as (e.g. Ma et al. 2012)

$$Pe = \frac{c_{pw} v_D l}{\lambda_m} \tag{2}$$

where c_{pw} is the volumetric heat capacity of water (c_{pw}=4.2×10^{6} J m^{-3} K^{-1}), v_D the Darcy velocity and l the characteristic length, which is a length specifying changes in the temperature (e.g. here total length of the observation well transect with 7.5 m).

The importance of considering density effects can be evaluated by calculating the ratio between the vertical buoyancy force and the horizontal friction force from regional groundwater flow. Oostrom et al. (1992) defined a stability number G as

$$G = \frac{K\frac{\Delta\rho}{\rho_0}}{v_D} = \frac{\Delta\rho}{i\rho_0} \tag{3}$$

where i is the hydraulic gradient, ρ_0 is the reference density of the thermally undisturbed aquifer and $\Delta\rho$ is the induced density difference. Oostrom et al. (1992) experimentally determined a critical value of G_c=0.3, where the transition from a stable to an unstable plume sets in.

Results and discussion

During the TTT, the vertical temperature profiles were recorded for 4 days in the injection well B2 and in the five downgradient observations wells (OW1–5). The measurements are shown in Fig. 5 as thermoisopleth graphs, which visualize the time-dependent evolution of the temperatures in the Lauswiesen aquifer cross-sections. In the same manner, the results of the numerical simulation are presented in Fig. 6. In the following, first the calibration of the numerical model is presented and then the temperature development at the injection well is discussed and the effects of hydraulic heterogeneity and induced density differences are examined. Next, the heat transport in the down gradient observation wells is discussed in more detail. Finally, the findings of the TTT are compared to those from previous DPIL measurements.

Calibration of the numerical model

For the calibration, the mean, minimal and maximal values of the uncertain flow and transport parameters of the two aquifer layers K, λ_m, c_{pm}, and α_L were considered. Preliminary testing revealed that simulated results are least sensitive to the thermal properties and strongly controlled by the hydraulic conductivity. Consequently, thermal properties and dispersivity, which are not expected to substantially vary in the aquifer, were assumed to be the same for both aquifer layers. The hydraulic conductivities were individually calibrated for each layer. Thus, 3^4 = 81 value combinations were tested, and the best fit between simulated and measured groundwater temperatures at injection and observation wells during the TTT was chosen for further analysis (Table 3).

For the thermal transport parameters of the aquifer, α_L= 0.68 m, c_{pm}=2.5×10^{6} J m^{-3} K^{-1}, and λ_m=2.7 W m^{-1} K^{-1} were derived. The obtained hydraulic conductivity of the more conductive upper aquifer layer is 8.9×10^{-3} m s^{-1} and the value of the lower one is 4.5×10^{-4} m s^{-1}. The model with this parameter set results in a root mean squared error (RMSE), between all simulated and measured BTCs, of 0.65°C. This misfit highlights that the numerical model may capture the main thermal transport processes in the aquifer, but is not capable of fully reproducing the observed temperature evolution, which is comprehensively discussed in the following sections.

 DOI 10.1007/s10040-013-1059-z

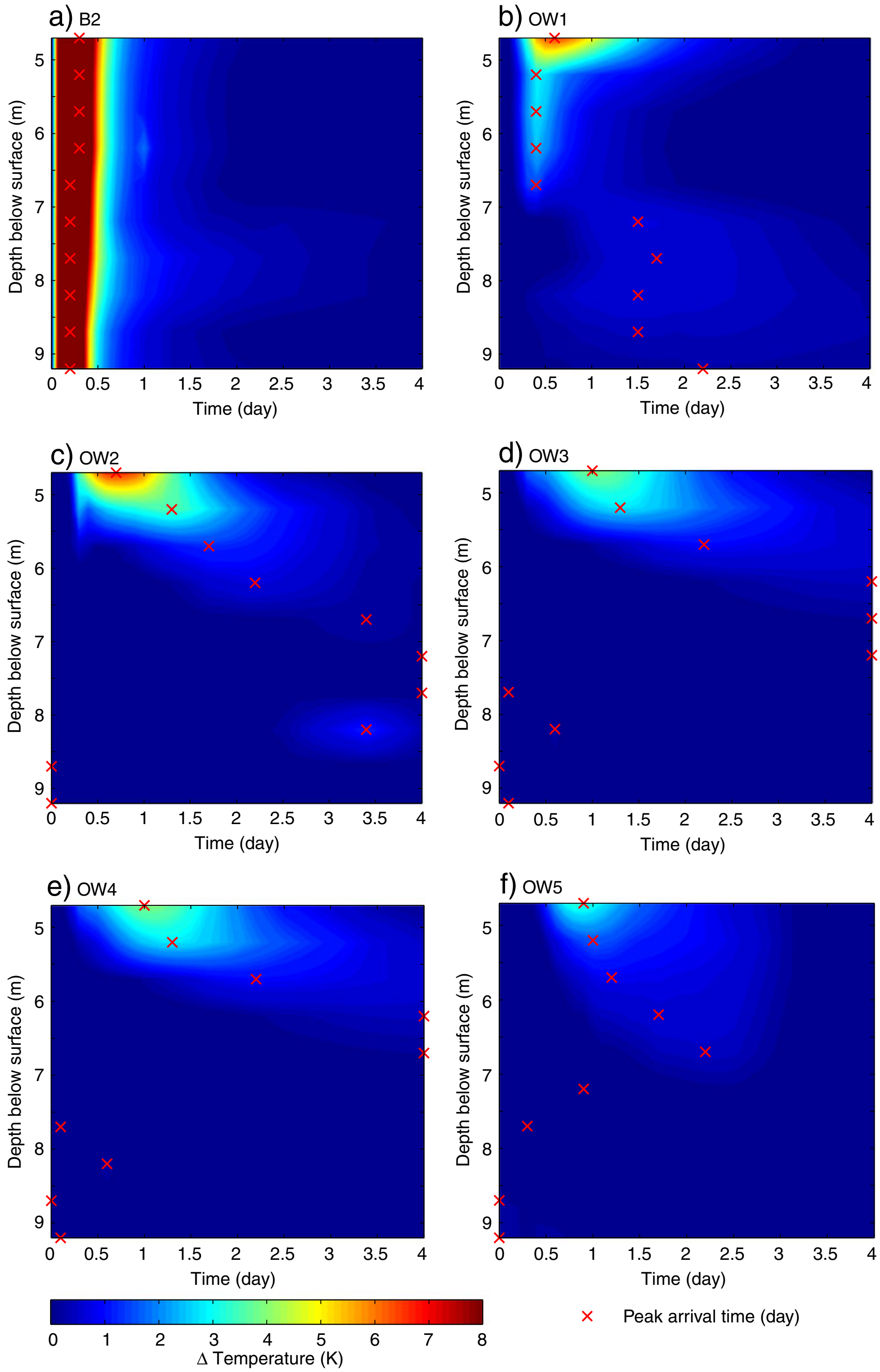

Fig. 5 Measured depth-related temperature development over the entire experimental period. The temperature change is calculated based on the initial temperature at the start of the experiment. Additionally, temperature peak arrival times for every measurement location are emphasized: **a** injection well B2; **b**–**f** observation wells OW1–5. For interpolation, the MATLAB®-function `contourc` is used

Temperature evolution at injection well

First, the temperature evolution at the injection well B2 is inspected. The temperature changes measured are illustrated in Fig. 5a. Small vertical variability indicates that a homogenized line-source with a temperature of 22.4±0.5°C (ΔT=11.4 K) was created below

 DOI 10.1007/s10040-013-1059-z

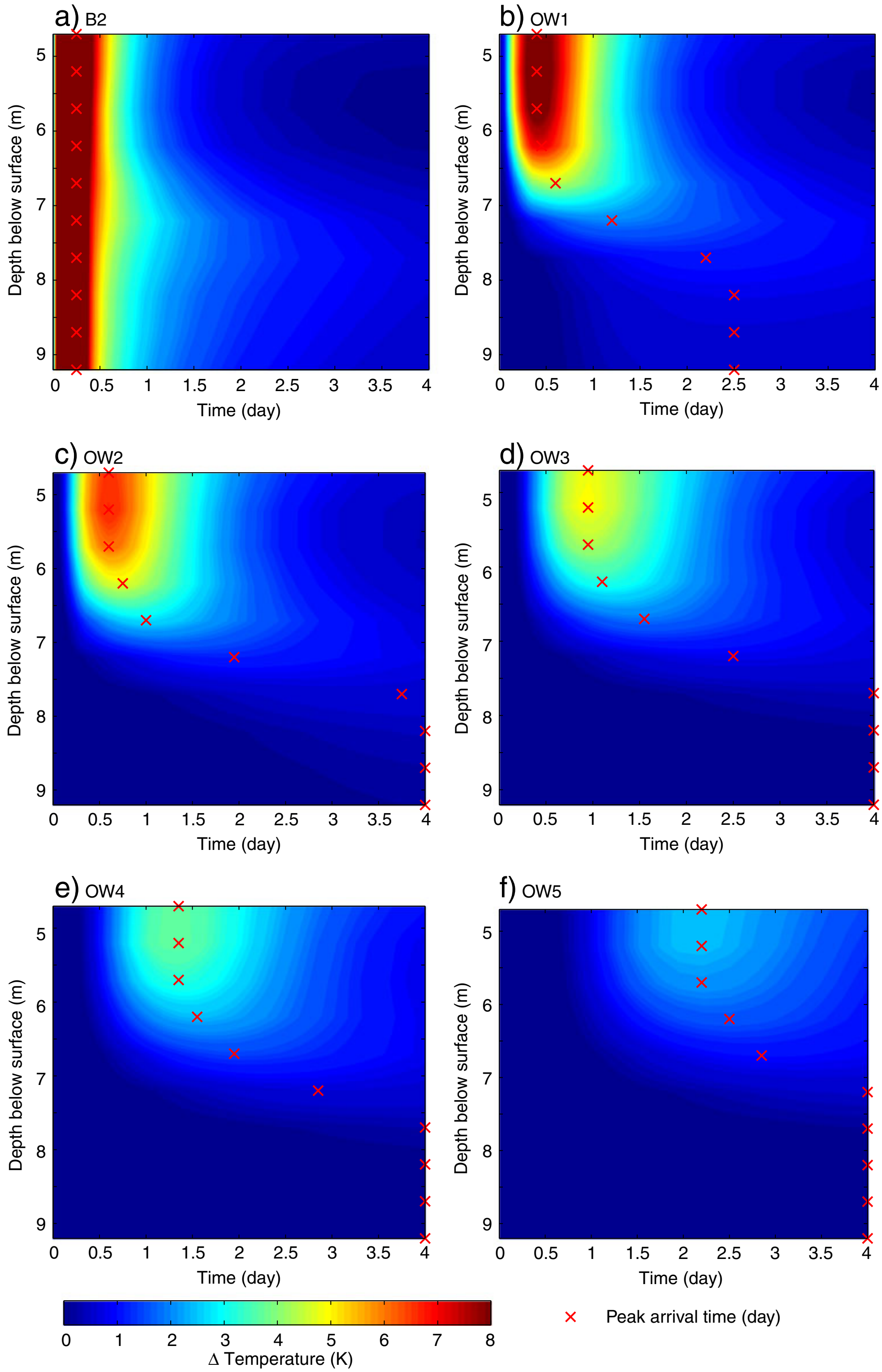

Fig. 6 Simulated depth related temperature development over the entire experimental period using the numerical heat-transport model. The temperature change is calculated based on the initial temperature at the start of the experiment. Additionally, temperature peak arrival times for every measurement location are emphasized: **a** injection well B2; **b**–**f** observation wells OW1–5. For interpolation, the MATLAB®-function `contourc` is used

the water table during the injection experiment (t<0.33 day). Proper mixing of the injected thermal tracer and the groundwater in and around the well was achieved, and after the warm water injection, only a slight vertical variability in the temperature is observed. Even if this variability is only marginal, it can

DOI 10.1007/s10040-013-1059-z

be seen that long-term cooling is most pronounced at the bottom, and highest temperatures appear in the lower section at about 7.2 m bls. This pattern of the temperature signal could be interpreted as a first indication of non-uniform horizontal groundwater movement with lower advective flow velocity in the lower part of the aquifer. Minor long-term cooling at the bottom may be attributed to slight vertical heat loss due to conduction into the aquitard beneath.

The numerical simulation for B2 shows a very similar development of the temperature in the injection well (Fig. 6a). However, a closer look reveals that after the injection, the thermal anomaly is more persistent. A possible explanation for this observation is that the assumption of a thermal equilibrium between solid and fluid phase in the numerical model, is not instantaneous in the vicinity of the injection well. Hence, less heat is stored in the subsurface than expected, based on the simulation, particularly during the fast injection of the warm water. As a consequence, cooling rates observed in the experiment exceed those in the thermally equilibrated simulations (Fig. 6a). After 1 day, increased temperatures are still apparent in the model, especially at the central and lower profiles. There is a temperature maximum in the injection well at a depth of around 7.2–7.7 m bls (Fig. 6a). Apparently, as observed in the field and in the model, the aquitard (and lower aquifer layer) temporally stores and slowly releases thermal energy at the injection well.

Density effects vs. hydraulic heterogeneity

Due to layering of the aquifer, advective forces in the more permeable layer dictate and focus thermal breakthrough in the upper part of the aquifer, which is confirmed by applying the values used for the calibrated numerical model to calculate the layer-specific Peclet numbers, Pe (Table 3, Eq. 2). For the upper part of the aquifer, Pe=420 and for the lower part, Pe=21; therefore, heat transport in both parts of the aquifer is dominated by advection, but it is more pronounced in the upper part. In comparison, for the aquitard, Pe is only 9×10^{-5}, indicating conduction dominated conditions in the aquitard.

The next observation well in the regional groundwater flow direction, OW1, positioned just 1.5 m downgradient of the injection well, reveals that the moving warm water only leaves a trace in the upper layer of the aquifer with a peak value of ΔT_{peak}=6.6 K (Fig. 5b). In comparison, with the numerical model (Fig. 6b), significant temperature changes are only detected in the uppermost part of the aquifer. At first sight, this observation may be a sign of density effects. However, following previous studies by, for example, Hecht-Méndez et al. (2010), Ma and Zheng (2010), Ma et al. (2012) and Leaf et al. (2012), such effects are expected to be negligible given the small temperature range and the short duration of the performed TTT experiment. Hence, a more plausible reason could be hydraulic heterogeneities within the upper layer with highest advection on top of the profile.

Further insight provides the stability criterion, G_c, according to Oostrom et al. (1992). Based on a groundwater density of 999.6 kg m^{-3} for 11°C, and an undisturbed hydraulic gradient of i=0.003, a maximum possible density change of 0.9 kg m^{-3} would be acceptable to avoid buoyancy effects ($G \leq G_c$=0.3). During the TTT at the Lauswiesen site, the maximal density change by temperature increase from 11 to 17°C is $\Delta\rho$= 0.9 kg m^{-3}. Consequently, the resulting value of G=0.3 indicates that density effects could not be completely ruled out (Eq. 3). However, temporary warm water infiltration yields transient conditions with a head build up at the injection well, and thus during injection, the local hydraulic gradient is increased at the injection well B2 (i>0.003). As a result, the maximum ΔT can be expected to be higher than the limit of ΔT=6 K obtained from a calculated density difference based on Eq. 3 for undisturbed flow conditions. Furthermore, flow field changes are most pronounced very close to the injection well and, even under well-controlled experiments, induced small-scale lateral and vertical flow components may be significant. Since hydraulic heads have not been continuously monitored during the experiment, clear quantitative evidence from the field cannot be provided.

Downgradient propagation of the thermal plume

The focus of the thermal plume in the uppermost part of the well is also observed in the more downgradient observation wells. Accordingly, the numerical model overestimates the vertical extension of the plume throughout the experiment. These observations may be influenced by measurement inaccuracies. The experiment is possibly prone to technical artifacts, like intra borehole convection, which is not considered in the numerical simulation either. Slight vertical warm water flow in the wells could have smeared the plume. Therefore, caution is given when interpreting the measured temperature trends at the wells. In further analysis, the peak arrival time is favored as a potentially more robust criterion. The values of t_{peak} are marked as red crosses in Figs. 5 and 6 for each sensor position.

The lower aquifer has a lower hydraulic conductivity, assuming that differences in pronounced t_{peak} are mainly controlled by different horizontal advective flow velocities. Thermal effects are minimal in the lower part of the aquifer (6–10 m bls). As a consequence of the small signal-to-noise ratio, the t_{peak} in the lower part the aquifer cannot be well determined, which is in line with the simulated results. The model predicts (Fig. 6) here that during the TTT, no thermal peak passes OW2–5, because obtained t_{peak} values are at the end of the experiment.

Under ideal conditions, the result of a TTT would show later t_{peak} values for the more downgradient wells with a decrease of ΔT_{peak}. Advection would move the peaks in the upper layer in the flow direction from OW1 to OW5, and diffusion and mechanical dispersion would lead to a longitudinal thermal plume spreading and transversal heat loss. This ideal transport behavior can be seen in the

 DOI 10.1007/s10040-013-1059-z

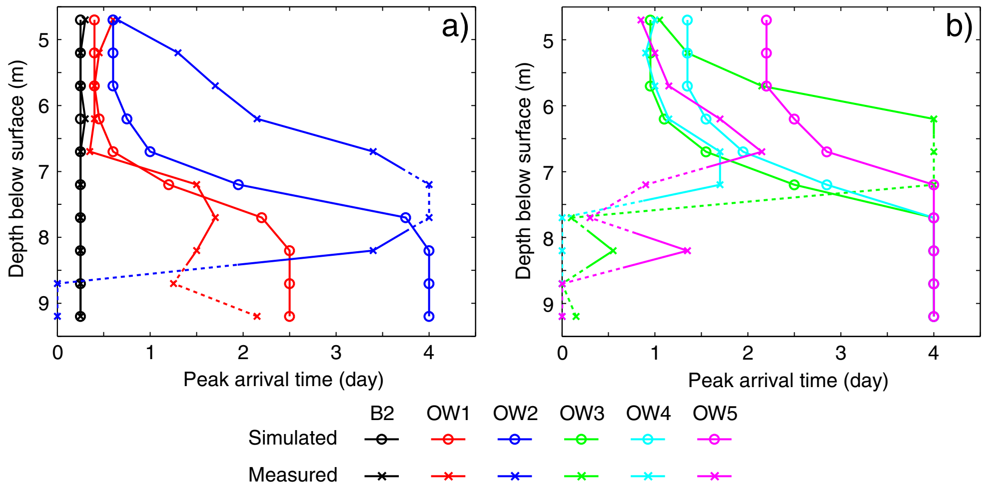

Fig. 7 Comparison of the peak arrival times (t_{peak}) measured and simulated for the TTT experiment. **a** B2, OW1 and OW2; **b** OW3–5. Dashed lines indicate uncertain sections, influenced by measurement inaccuracies or data noise (ΔT_{peak}<0.3 K)

numerical simulation (Fig. 6). There is a gradual decline of the numerically obtained peak temperatures with increasing distance of observation well from injection well. For example, the temperature differences at a depth 4.7 m bls are ΔT=8.5 K (OW1) to 6.6 K (OW2), 4.9 K (OW3), 3.8 K (OW4), and 2.5 K (OW5).

The measured temperature values follow a similar trend as those simulated by the model, but with some deviations. As expected, temperature differences are least pronounced at the most distant observation well OW5 (Fig. 5f). Measured and simulated t_{peak} agree well in the closest OW1. However, there is no gradual decline in the wells closer to the injection well. Peak temperatures on top of the screened section (4.7 m bls) change from ΔT= 6.6 K (OW1) to 6.8 K (OW2), 4.0 K (OW3), 4.7 K (OW4), and 3.3 K (OW5). Furthermore, peak arrival times recorded at the upper sensor do not increase with distance.

The evolution of the thermal plume measured during the TTT and values of t_{peak} provide crucial hints that substantial spatial heterogeneity are present in the aquifer, which is insufficiently reproduced in the model by two horizontal and laterally persistent layers. Small-scale, vertical heterogeneity has already been identified as a potential reason that the plume is detected only in the uppermost well screens. In the upper part of the aquifer, at OW2 and OW3, t_{peak} trends would compare better by simple shifting along the vertical axis. This shift could be an indication that the boundary between the upper and the lower aquifer part is declined or displaced relative to the assumptions in the model. The inconsistencies in t_{peak} between model and field of OW4 and OW5 are a sign of lateral heterogeneities in the direction of the well transect, as well as perpendicular. The thermal plume appears locally deviated from the suspected centerline, potentially with meandering. Thus, the measured temperatures may originate from the fringe of the thermal plume. This conclusion is supported by the measured t_{peak} values at OW4 and OW5, which are smaller than those at OW3, meaning that the thermal peak arrives at OW4 and OW5 before it passes OW3.

Comparison to DPIL

Finally, t_{peak} values are compared to the DPIL profiles (Figs. 3 and 7). The overall patterns are comparable, and both field experiments are obviously consistent with higher relative hydraulic conductivities and smaller t_{peak} values in the upper part of the aquifer. The 6 m bls boundary between both aquifer parts in the DPIL-profile of B2 is well reproduced by the model. The DPIL-profiles of OW4 and OW5 indicate that this boundary could be at a more shallow depth, which corresponds to the interpretation from trends in the t_{peak} values. Due to the substantial influence of noise on the small values shown on logarithmic scale, the DPIL-based characterization of the lower section is as unsatisfactory as from the TTT. Further insights in the heat transport characteristics of the studied aquifer would mandate an even denser measurement network and a longer duration of TTT observation to assure the monitoring of the passage of the thermal peak.

Conclusions

The main objective of the TTT at the Lauswiesen site was to improve understanding of the results from the experiment and, with the obtained experience, identify implications for future TTT designs. By numerical simulation of the TTT, the governing transport processes could be identified, and high-conductivity regions at the top of the aquifer could also be confirmed. The heterogeneous hydraulic properties of the studied shallow aquifer, which is generally well known and has already served as a hydrogeological test case for decades, have substantial effects on the heat transport behavior. It is shown that macrodispersion and flow-focusing occurred, and that

 DOI 10.1007/s10040-013-1059-z

complex flow patterns result in thermal breakthrough curves (shown as thermoisopleth graphs) that are substantially distinct from what would be expected under ideal conditions in a layered aquifer. Accordingly, the capability of the presented model to simulate the measured propagation of the thermal plume is limited. For more comprehensive flow and transport simulations, however, the data collected during this experiment are insufficient. A main obstacle is that the induced transient hydraulic head change at injection well and in the observation wells were not continuously monitored during the experiment. Hence, piezometers have to be added to the experimental design, especially, when the injected water volume per time is significant in comparison to the anticipated natural groundwater flow.

Considering that lateral and even vertical flow and transport components may be significant in such highly heterogeneous systems, it is also recommended to use a more distributed and space-filling arrangement of observation wells (e.g. several observation well transects) than the linear one chosen in the performed TTT. Such wells, which also reveal the thermal evolution aside from the expected dominant flow direction, show valuable insights in the 3D characteristics of the transport mechanisms. Furthermore, particularly in the case of long-duration experiments, sensors are needed that monitor potential vertical conductive heat losses such as into the underlying aquitard and the unsaturated zone above.

Ideally, the TTT is complemented by additional field experiments such as near surface geophysics (e.g. Slater 2007) or hydraulic tomography (e.g. Brauchler et al. 2013), which are able to identify the main structural build-up of the aquifer. For example, at the Lauswiesen site, DPIL field tests have been performed before the TTT. It is demonstrated that the monitored thermal transport along the local hydraulic gradient is consistent with the findings from the DPIL campaign. In addition, as reported by Ma et al. (2012), injection of both thermal and dye tracers is an appealing combination, which should be considered for future active and short-term TTT. Thus, coupled parameter estimation for determining both thermal and solute transport parameters would be possible (Rau et al. 2012), which would better constrain the inversion problem than by separate interpretation of individual tracer tests. Although heat appears to be a favorable tracer for studying aquifer properties, care has to be taken to interpret the acquired data. Hence, more studies on active and short-term TTT are required to establish such tests as a standard hydrogeological investigation technique.

Acknowledgements This research was supported by the Swiss National Science Foundation (SNSF) under grant number 200021L 144288, and the German Research Foundation (DFG), under grant number BL 1015/4-1. We are also grateful to Uwe Schneidewind and Wolfgang Kürner for their support during the field campaign and two anonymous reviewers for their fruitful comments.

References

Anderson MP (2005) Heat as a ground water tracer. Ground Water 43(6):951–968

Bellin A, Rubin Y (2004) On the use of peak concentration arrival times for the inference of hydrogeological parameters. Water Resour Res 40(7):1–13

Bou Ghannam O (2006) Determination of the hydraulic conductivity using direct-push methods. MScThesis, University of Tübingen, Germany

Brauchler R, Hu R, Hu L, Jiménez S, Bayer P, Dietrich P, Ptak T (2013) Rapid field application of hydraulic tomography for resolving aquifer heterogeneity in unconsolidated sediments. Water Resour Res 49(4):2013–2024

Bravo HR, Jiang F, Hunt RJ (2002) Using groundwater temperature data to constrain parameter estimation in a groundwater flow model of a wetland system. Water Resour Res 38(8):1–14

Brouyère S, Carabin G, Dassargues A (2004) Climate change impacts on groundwater resources: modelled deficits in a chalky aquifer, Geer basin, Belgium. Hydrogeol J 12(2):123–134

Butler JJ, Healey JM, McCall GW, Garnett EJ, Loheide SP (2002) Hydraulic tests with direct-push equipment. Ground Water 40(1):25–36

Clauser C (2011) Thermal storage and transport properties of rocks, I: heat capacity and latent heat. In: Gupta H (ed) Encyclopedia of solid earth geophysics. Springer, Netherlands, pp 1423–1431

Conant B (2004) Delineating and quantifying ground water discharge zones using streambed temperatures. Ground Water 42(2):243–257

Constantz J (2008) Heat as a tracer to determine streambed water exchanges. Water Resour Res 44(4):1–20

Diersch H-JG (2009) FEFLOW reference manual. WASY GmbH, Berlin

Dietrich P, Butler JJ, Faiß K (2008) A rapid method for hydraulic profiling in unconsolidated formations. Ground Water 46(2):323–328

Domenico PA, Schwartz FW (1998) Physical and chemical hydrogeology, 2nd edn. Wiley, Chichester, UK

Doussan C, Toma A, Paris B, Poitevin G, Ledoux E, Detay M (1994) Coupled use of thermal and hydraulic head data to characterize river-groundwater exchanges. J Hydrol 153(1–4):215–229

Engelhardt I, Prommer H, Moore C, Schulz M, Schüth C, Ternes TA (2013) Suitability of temperature, hydraulic heads, and acesulfame to quantify wastewater-related fluxes in the hyporheic and riparian zone. Water Resour Res 49:1–15

Ferguson G, Woodbury AD (2007) Urban heat island in the subsurface. Geophys Res Lett 34(23):1–4

Händel F, Dietrich P (2012) Relevance of deterministic structures for modeling of transport: the Lauswiesen case study. Ground Water 50(6):935–942

Hecht-Méndez J, Molina-Giraldo N, Blum P, Bayer P (2010) Evaluating MT3DMS for heat transport simulation of closed geothermal systems. Ground Water 48(5):741–756

Jardani A, Revil A (2009) Stochastic joint inversion of temperature and self-potential data. Geophys J Int 179(1):640–654

Keery J, Binley A, Crook N, Smith JWN (2007) Temporal and spatial variability of groundwater–surface water fluxes: development and application of an analytical method using temperature time series. J Hydrol 336(1–2):1–16

Keys WS, Brown RF (1978) The Use of temperature logs to trace the movement of injected water. Ground Water 16(1):32–48

Kocabas I (2005) Geothermal reservoir characterization via thermal injection backflow and interwell tracer testing. Geothermics 34(1):27–46

Kollet SJ, Cvijanovic I, Schüttemeyer D, Maxwell RM, Moene AF, Bayer P (2009) The influence of rain sensible heat and subsurface energy transport on the energy balance at the land surface. Vadose Zone J 8(4):846–857

Leaf AT, Hart DJ, Bahr JM (2012) Active thermal tracer tests for improved hydrostratigraphic characterization. Ground Water 50(5):726–735

Lessoff SC, Schneidewind U, Leven C, Blum P, Dietrich P, Dagan G (2010) Spatial characterization of the hydraulic conductivity using direct-push injection logging. Water Resour Res 46(12):1–9

Lowry CS, Walker JF, Hunt RJ, Anderson MP (2007) Identifying spatial variability of groundwater discharge in a wetland stream using a distributed temperature sensor. Water Resour Res 43(10):1–9

Ma R, Zheng C (2010) Effects of density and viscosity in modeling heat as a groundwater tracer. Ground Water 48(3):380–389

Ma R, Zheng C, Zachara JM, Tonkin M (2012) Utility of bromide and heat tracers for aquifer characterization affected by highly transient flow conditions. Water Resour Res 48(8):1–18

Macfarlane A, Förster A, Merriam D, Schrötter J, Healey J (2002) Monitoring artificially stimulated fluid movement in the Cretaceous Dakota aquifer, western Kansas. Hydrogeol J 10(6):662–673

Markle JM, Schincariol RA, Sass JH, Molson JW (2006) Characterizing the two-dimensional thermal conductivity distribution in a sand and gravel aquifer. Soil Sci Soc Am J 70(4):1281–1294

Menberg K, Bayer P, Zosseder K, Rumohr S, Blum P (2013) Subsurface urban heat islands in German cities. Sci Total Environ 442:123–133

Molina-Giraldo N, Bayer P, Blum P (2011a) Evaluating the influence of thermal dispersion on temperature plumes from geothermal systems using analytical solutions. Int J Therm Sci 50(7):1223–1231

Molina-Giraldo N, Bayer P, Blum P, Cirpka OA (2011b) Propagation of seasonal temperature signals into an aquifer upon bank infiltration. Ground Water 49(4):491–502

Molson JW, Frind EO, Palmer CD (1992) Thermal energy storage in an unconfined aquifer: 2. model development, validation, and application. Water Resour Res 28(10):2857–2867

Molz FJ, Melville JG, Parr AD, King DA, Hopf MT (1983) Aquifer thermal energy storage: a well doublet experiment at increased temperatures. Water Resour Res 19(1):149–160

Neuman SP (1990) Universal scaling of hydraulic conductivities and dispersivities in geologic media. Water Resour Res 26(8):1749–1758

Oostrom M, Hayworth JS, Dane JH, Güven O (1992) Behavior of dense aqueous phase leachate plumes in homogeneous porous media. Water Resour Res 28(8):2123–2134

Palmer CD, Blowes DW, Frind EO, Molson JW (1992) Thermal energy storage in an unconfined aquifer: 1. field injection experiment. Water Resour Res 28(10):2845–2856

Parr AD, Molz FJ, Melville JG (1983) Field determination of aquifer thermal energy storage parameters. Ground Water 21(1):22–35

Pehme P, Parker BL, Cherry JA, Molson JW, Greenhouse JP (2013) Enhanced detection of hydraulically active fractures by temperature profiling in lined heated bedrock boreholes. J Hydrol 484:1–15

Rath V, Wolf A, Bücker HM (2006) Joint three-dimensional inversion of coupled groundwater flow and heat transfer based on automatic differentiation: sensitivity calculation, verification, and synthetic examples. Geophys J Int 167(1):453–466

Rau GC, Andersen MS, Acworth RI (2012) Experimental investigation of the thermal dispersivity term and its significance in the heat transport equation for flow in sediments. Water Resour Res 48(3):1–21

Read T, Bour O, Bense V, Le Borgne T, Goderniaux P, Klepikova MV, Hochreutener R, Lavenant N, Boschero V (2013) Characterizing groundwater flow and heat transport in fractured rock using fiber-optic distributed temperature sensing. Geophys Res Lett 40(10):2055–2059

Rein A, Hoffmann R, Dietrich P (2004) Influence of natural time-dependent variations of electrical conductivity on DC resistivity measurements. J Hydrol 285(1–4):215–232

Riva M, Guadagnini L, Guadagnini A, Ptak T, Martac E (2006) Probabilistic study of well capture zones distribution at the Lauswiesen field site. J Contam Hydrol 88(1–2):92–118

Saar M (2011) Review: geothermal heat as a tracer of large-scale groundwater flow and as a means to determine permeability fields. Hydrogeol J 19(1):31–52

Sack-Kühner B (1996) Establishing the natural test site "Lauswiesen Tübingen". Diploma Thesis, University of Tübingen, Germany

Sauty JP, Gringarten AC, Fabris H, Thiery D, Menjoz A, Landel PA (1982a) Sensible energy storage in aquifers: 2. field experiments and comparison with theoretical results. Water Resour Res 18(2):253–265

Sauty JP, Gringarten AC, Menjoz, Landel PA (1982b) Sensible energy storage in aquifers: 1. theoretical study. Water Resour Res 18(2):245–252

Schmidt C, Bayer-Raich M, Schirmer M (2006) Characterization of spatial heterogeneity of groundwater-stream water interactions using multiple depth streambed temperature measurements at the reach scale. Hydrol Earth Syst Sci 10(6):849–859

Schneidewind U (2008) Determination of the hydraulic conductivity using Direct-Push Injection Logger. MSc Thesis, University of Tübingen, Germany

Shook GM (1999) Prediction of thermal breakthrough from tracer tests. Paper presented at the 24th Workshop on Geothermal Reservoir Engineering, Stanford, CA, January 1999

Shook GM (2001) Predicting thermal breakthrough in heterogeneous media from tracer tests. Geothermics 30(6):573–589

Slater L (2007) Near surface electrical characterization of hydraulic conductivity: from petrophysical properties to aquifer geometries—a review. Surv Geophys 28(2–3):169–197

Taniguchi M, Shimada J, Tanaka T, Kayane I, Sakura Y, Shimano Y, Dapaah-Siakwan S, Kawashima S (1999) Disturbances of temperature-depth profiles due to surface climate change and subsurface water flow: 1. an effect of linear increase in surface temperature caused by global warming and urbanization in the Tokyo Metropolitan Area, Japan. Water Resour Res 35(5):1507–1517

Taniguchi M, Turner JV, Smith AJ (2003) Evaluations of groundwater discharge rates from subsurface temperature in Cockburn Sound, Western Australia. Biogeochemistry 66(1–2):111–124

Vandenbohede A, Louwyck A, Lebbe L (2008a) Identification and reliability of microbial aerobic respiration and denitrification kinetics using a single-well push–pull field test. J Contam Hydrol 95(1–2):42–56

Vandenbohede A, Van Houtte E, Lebbe LUC (2008b) Study of the feasibility of an aquifer storage and recovery system in a deep aquifer in Belgium. Hydrol Sci J 53(4):844–856

Vandenbohede A, Louwyck A, Lebbe L (2009) Conservative solute versus heat transport in porous media during push-pull tests. Transport Porous Media 76(2):265–287

Vogt T, Schneider P, Hahn-Woernle L, Cirpka OA (2010) Estimation of seepage rates in a losing stream by means of fiber-optic high-resolution vertical temperature profiling. J Hydrol 380(1–2):154–164

Wu X, Pope GA, Shook GM, Srinivasan S (2008) Prediction of enthalpy production from fractured geothermal reservoirs using partitioning tracers. Int J Heat Mass Transf 51(5–6):1453–1466

Xue Y, Xie C, Li Q (1990) Aquifer thermal energy storage: a numerical simulation of field experiments in China. Water Resour Res 26(10):2365–2375

Ziagos JP, Blackwell DD (1986) A model for the transient temperature effects of horizontal fluid flow in geothermal systems. J Volcanol Geotherm Res 27(3–4):371–397

 DOI 10.1007/s10040-013-1059-z